

Ectopic Expression of a Bamboo *SVP*-Like Gene Alters Flowering Time and Floral Organs in *Arabidopsis Thaliana*

Shinan Liu

Guangxi University

Naresh Vasupalli

Zhejiang Agriculture and Forestry University

Dan Hou

Zhejiang Agriculture and Forestry University

Xinchun Lin (✉ linxcx@163.com)

Zhejiang Agriculture and Forestry University <https://orcid.org/0000-0003-0168-331X>

Research Article

Keywords: Phyllostachys violascens, PvSVP2, flowering time, ectopic expression, functional analysis, E. coli

Posted Date: January 18th, 2022

DOI: <https://doi.org/10.21203/rs.3.rs-1245022/v1>

License:   This work is licensed under a Creative Commons Attribution 4.0 International License.

[Read Full License](#)

Abstract

The *Short Vegetative Phase (SVP)* gene is a key regulator for floral transition and development. Although *SVP*-like genes have been identified and characterized in many plant species, their orthologs in bamboo have not been characterized. In this study, one *SVP* homolog was isolated from lei bamboo based on the *P. edulis* transcriptome database and designated as *PvSVP2*. Phylogenetic analysis showed that *PvSVP2* was closely related to rice *OsMADS47*. Expression analysis revealed that *PvSVP2* was widely expressed in different tissues but significantly in vegetative tissues. Moreover, it has higher transcript levels in the late stages of flower development. Overexpression of *PvSVP2* in *Arabidopsis thaliana* caused the early flowering and abnormal floral morphologies. Further, the qRT-PCR analysis showed that the genes regulating flowering time (*FT* and *SOC1*) and flower development (*AP1*, *AP3* and *PI*) expressions were significantly increased in transgenic *A. thaliana* lines and correlated with *PvSVP2* expression. The subcellular location of *PvSVP2* in both onion epidermal cells and *A. thaliana* protoplast was localized in the nucleus and cytomembrane. Through yeast two-hybrid and BIFC assays, we identified that *PvSVP2* interact with *PvMADS56* (a *SOC1* homolog) and *PvVRN1* (an *AP1* homolog). These results suggested that *PvSVP2* may play an essential role in the flowering process of bamboo by regulating the *PvMADS56* and *PvVRN1*. Besides, we purified and obtained the *PvSVP2* recombinant protein by prokaryotic inducement. Our data will provide information to understand the characterization and function of *PvSVP2* and be beneficial to illustration the molecular mechanism of bamboo flowering.

Key Message

PvSVP2, a bamboo *SVP* homolog, might cause early flowering and abnormal floral organs by interacting with *PvMADS56* and *PvVRN1*.

Introduction

The floral transition is a complex process and significantly affects both plant fitness and crop yield. Therefore studying the underlying mechanisms is vital for increasing agricultural productivity (Bouché et al. 2016). The *Short Vegetative Phase (SVP)* gene is a crucial flowering repressor and regulated by autonomous, thermosensitive and gibberellin pathways (Andrés et al., 2014; Hartmann et al. 2000; Lee et al. 2013; Li et al. 2008; Marín-González et al. 2015). Although *SVP* is widely expressed in plant stems and leaves, it can delay the floral transition by regulating integrators of flowering time signals (*SOC1*, *FT* and *FLC* genes) (Li et al. 2008; Jang et al. 2009; Mateos et al. 2015). The integrators integrate various environmental and endogenous signals to control the transition from vegetative to reproductive development (Bouché et al. 2016; Amasino and Michaels 2010; Parcy 2005). In addition, *SVP* also interacts directly or indirectly with *AP1*, *AP3*, *PI* and *SEP3* to affect the development of floral organs (Gregis et al. 2006; de Folter et al. 2004). Therefore, *SVP* not only controls the flowering time but also affects flower development.

The role of *SVP* genes in flower development and flowering time regulation, consistent in most of the studies. In *A. thaliana*, overexpression of *SVP* genes leads to late flowering and *svp* mutant plants were early flowering (Bouché et al. 2016; Li et al. 2008; Masiero et al. 2004). Ectopic expression of *PtSVP* from trifoliolate orange in *A. thaliana* causes late flowering and additional trichomes and floral defects (Li et al. 2010). Overexpression of two *Medicago* *SVP* genes causes floral defects and delayed flowering in *A. thaliana* (Jaudal et al. 2014). In kiwifruit, four *SVP* (*SVP1*, *SVP2*, *SVP3* and *SVP4*) homologs have been identified. Among them, *SVP1* and *SVP3* act repressors of flowering and the overexpression studies identify that these gene was able to rescue the *A. thaliana* *svp-41* mutant (Wu et al. 2012). These data show that *SVP*-like genes have the conserved roles in dicot species in floral development and flowering time regulation. In *Antirrhinum*, *INCOMPOSITA* (an *SVP* homolog) controls prophyll development, floral meristem identity and flowering time (Masiero et al. 2004).

In contrast, *SVP* homologs from monocots mainly regulate flower development instead of flowering time. In barley (*Hordeum vulgare*), ectopic expression of *Barley MADS1* (*BM1*) and *BM10* (*SVP* homologs) inhibit floral development and cause floral reversion (Trevaskis et al. 2007). There are three *SVP*-like genes (*OsMADS22*, *OsMADS47* and *OsMADS55*) in rice (Lee et al. 2008a). Further, transgenic rice overexpressing *OsMADS22* have abrupt floral morphogenesis (a disorganized palea, an elongated glume and a two-floret spikelet) (Sentoku et al. 2005). Heterologous expression of *OsMADS22* and *OsMADS47* in *A. thaliana* only causes the alternation of flower development but not complement for the flowering phenotypes of *svp* mutant (Fornara et al. 2008). However, overexpression of *OsMADS55* delays the flowering time of wild-type plants and rescues the early flowering phenotype of *svp* mutant in *A. thaliana* (Lee et al. 2012). Above results indicated that *SVP* homologs in plants were multifunctional genes along with conservative and divergent characteristics.

Bamboo is the woody monocot that belongs to the grass family Poaceae (Hou et al. 2021). However, bamboo is semelparous and owns many peculiar habits in flowering (Lin and Mao 2007). Bamboo flowering has a long vegetative phase and is unpredictable. Further, the flowering intervals vary from a few years to several decades (Sharma et al. 2014; Yao et al. 2020; Zheng et al. 2020). The flowering is often followed by the death of the flowered clumps (Lin and Mao 2007; Hou et al. 2020). The gregarious bamboo flowering results in substantial economic loss and ecological crisis in many tropical and subtropical regions. The mechanism of bamboo flowering is still unknown, even if this phenomenon has been recorded and studied for a long time. The *SVP*-like genes from monocots and dicots play an important role in the regulation of flowering. However, the molecular characteristics of bamboo *SVP*-like genes and their functions are still unclear. In this study, an *SVP*-like gene from lei bamboo (*Phyllostachys violascens*) was cloned and characterized by analyzing the overexpression plants of transgenic *A. thaliana*. Our study will lay a foundation to understand the mechanism of bamboo flowering.

Materials And Methods

Plant material and growth conditions

Lei bamboo samples used for gene cloning and expression analysis were collected in the Bamboo Garden of Zhejiang A and F University. Wild-type *A. thaliana* Columbia-0 (Col-0) was used for gene transformation. Seeds were sterilized with 10% sodium hypochlorite (NaClO) and washed five times with ddH₂O, and then sowed onto 1/2 MS petri dish. The *A. thaliana* seedlings were transplanted into the soil when they grew four cotyledons. All *A. thaliana* plants grow at 22°C under a long photoperiod (16h light /8h dark) in a control growth chamber.

Isolation of PvSVP2 from Lei bamboo

Total RNA was extracted from the young leaf using Trizol reagent (Invitrogen, US). RNA quality and concentration were detected with 1% RNase-free agarose/ethidium bromide gels and spectrophotometer. First-strand cDNA was synthesized by using Reverse Transcriptase M-MLV (TAKARA Company). The sequence of *OsMADS55* and *OsMADS47* (*SVP* homolog from rice) ORF were blasted on the moso bamboo (*P. edulis*) transcriptome database (Peng et al. 2013) by BioEdit software and isolated the *PvSVP1* (data not show in this paper) and *PvSVP2* genes. Full-length sequences were amplified using gene-specific primers of *PvSVP2* (Table S1). The PCR product was cloned into a pMD20-T vector (Takara Company) and then sequenced for further verification.

Plasmid construction and transformation of *A. thaliana*

To construct the overexpression vector, the ORF of *PvSVP2* was ligated to the *KpnI-Sall* site of the pCAMBIA1302 vector under the control of cauliflower mosaic virus (CaMV) 35S promoter. The *pCAMBIA1302-PvSVP2* fusion vector was transformed into *Agrobacterium tumefaciens* strain *GV3101* cells and then were introduced into *A. thaliana* (ecotype Col-0) using the floral dip method (Clough and Bent 1998). Transgenic seeds were survived in the medium containing 50 µg/ml hygromycin were transferred to soil and further confirmed by genomic PCR. Screened as above, positive T₃ generation of *35S::PvSVP2* transgenic *A. thaliana* were used for further study. The flowering time of *A. thaliana* was scored as rosette leaf number and days in which the main stem bolted 1cm.

Gene expression analyses

Quantitative real-time PCR (qRT-PCR) was used to analyze the spatio-temporal expression of *PvSVP2*. Total RNA was extracted from different tissues, including young leaf, mature leaf, culm, rhizome, shoot or flower, and at three times (young leaf and flower) as described by Liu et al. (2016) in flowering and non-flowering plants and healthy leaves of wild-type and T₃ homozygous transgenic plants. qRT-PCR reactions were performed in CFX96 Real-Time PCR Detection System (Bio-Rad, Germany) with SYBR Premix Ex Taq II mix (Takara). The PCR conditions were as follows: 95 °C for 3 min, followed by 40 cycles of amplification (95 °C for 10 sec, 60 °C for 20 sec). Reactions were performed in 20-µL mixtures consisting of 10 µL 2×SYBR Premix Ex Taq II mix, 0.5 µL each forward or reverse primer, 1 µL cDNA template and 8 µL ddH₂O. The *PheUBC18* gene from moso bamboo was used as the control for normalization (Qi et al. 2013) for different tissues expression analyses. The primers are listed in Table S1.

Further, *FLC*, *FT*, *SOC1*, *AP1*, *AP3* and *PI* genes expressions were also analyzed by gene-specific primers (Table S1) in wild-type and T₃ homozygous transgenic plants. The actin1 was used as an internal control. The relative gene expression levels were calculated using the $2^{-\Delta\Delta Ct}$ method (Livak and Schmittgen 2001).

Subcellular localization

To determine the subcellular location, the coding sequences of *PvSVP2* without TAG at the 3' end was ligated to the *BamHI-Sall* site of the vector Cam35S-gfp to generate a 35S::PvSVP2-GFP fusion vector. The plasmid 35S::PvSVP2-GFP was transfected into onion epidermal cells by particle bombardment method (Wang et al.1988) and *A. thaliana* protoplasts by the polyethylene glycol (PEG) as described by Yoo et al.(2007). Meanwhile, the transient expression of the empty vector (Cam35S-gfp) was used as a positive control. The corresponding fluorescence images were taken using a confocal laser scanning microscope (LSM510, Zeiss, Germany).

Yeast two-hybrid assay

The coding sequences of *PvSVP2*, *PvMADS56* and *PvVRN1* were amplified with specific primers (Table S1) and cloned into the pGADT7 (AD) and pGBKT7 (BD) plasmids. All the constructs were verified by sequencing. According to the manufacturer's instructions, the prey pGADT7 vector and constructs AD-PvSVP2, AD-PvVRN1, and AD-PvMADS56 were transformed into yeast strain Y2H Gold, and the bait pGBKT7 vector and constructs BD-PvSVP2, BD-PvVRN1, BD-PvMADS56 were transformed into yeast strain Y187. The transformed yeast cells were incubated at 30°C for 3-5 days on the selection medium SD/-Leu/X- α -gal and SD/-Trp/ X- α -gal for autoactivation. The cells that do not develop blue were confirmed as they do not contain autoactivation. The pGBKT7-53 + pGADT7-T and pGBKT7-Lam+ pGADT7-T were positive and negative controls, respectively. The protein interactions were confirmed on SD/-Trp/-Leu/-His/-Ade/ X- α -gal medium.

Bi-molecular fluorescence complementation (BIFC) analysis

The coding sequences of *PvSVP2*, *PvVRN1* and *PvMADS56* genes were cloned into pSAT1-nEYFP-C1 (nYFP) and pSAT4-cEYFP-C1(B) (cYFP) to generate PvSVP2-cYFP, PvVRN1-nYFP, PvMADS56-nYFP constructs. Protoplasts were isolated from the leaves of three-week-old *A. thaliana* plants. The pair plasmids of PvSVP2-cYFP/PvVRN1-nYFP, and PvSVP2-cYFP /PvMADS56-nYFP were cotransformed into *A. thaliana* protoplasts based on the polyethylene glycol (PEG) mediated transformation method described by Yoo et al. (2007). The plasmid combinations PvSVP2-cYFP/ pSAT1-nYFP, pSAT4-cYFP/PvVRN2-nYFP, pSAT4-cYFP /PvMADS56-nYFP were used as controls. The transformed cells images were captured after 20 h incubation in a confocal laser scanning microscopy (LSM510, Zeiss, Germany) at 488 nm excitation and 594 nm emission was observed.

Prokaryotic expression and purification of *PvSVP2*

The open reading frame of *PvSVP2* was amplified using pMD19-*PvSVP2* plasmid as the template and then linked to the *Bam*HI-*Sall* site of the vector pET-HTT (pHTT) to form a *PvSVP2*-pHTT fusion vector. The positive *PvSVP2*-pHTT construct was transformed into *E. coli* Rossetta TM (DE3) cell for protein production. The cells were cultivated in Luria-Bertani (LB) media containing 1% tryptone, 0.5% yeast extract, 1% NaCl and 50 mg/ml kanamycin. 10 ml bacteria was further inoculated into 1L LB culture at 37 °C for 220r/m until the OD600 reached to 0.5-0.6. Isopropyl-thiogalactoside (IPTG) was added with a final concentration of 400 μmmol/L while no IPTG as a control. Then the bacteria were induced under 37°C and 20°C for 5h and 12h, respectively. The cells were centrifuged at 5000×g for 10min. The collected precipitates were disrupted in lysis buffer with a 10min sonication at amplitude of 35% power (on/off 8/6 s). Then the supernatants and precipitates were separately collected and were detected by 12% sodium dodecylsulfate-polyacrylamide gel electrophoresis (SDS-PAGE).

Next, the *PvSVP2*-pHTT fusion protein was purified from the supernatant using the Dextrin Sepharose High performance (GE Company, Shanghai). The supernatant was added to 2 ml Nickel beads and rocked slowly on ice for 1 h after washing Nickel beads with the sterile distilled water and lyse buffer successively. The Nickel beads were then washed with 15 column volumes (CV) of lysis buffer with 40mmol/L concentration. *PvSVP2* protein was further eluted by 15 CV of lysis buffer, including 40mmol/L imidazole. The eluents were collected and analyzed by 12% SDS.

Bioinformatics and statistical analyses

The amino acid sequences of related SVP-like proteins used in phylogenetic tree construction were retrieved from the NCBI database. Phylogenetic analysis was constructed in the MEGA 5.0 software using the Neighbor-Joining method with a bootstrap value of 1000 replications (Tamura et al. 2011). Primers were designed by the Vector NTI and Premier Primer 5 software. The software ProtParam in the ExPASy (<http://expasy.org>) was used to analyze the physical and chemical properties of the protein. The subcellular localization of the protein was predicted with WoLF PSORT (http://www.genscript.com/psort/wolf_psort.html). Statistical analysis was carried out using SPSS 21.0. Differences were analyzed with one-way ANOVA followed by Tukey's test. Significance was accepted at the level of $p < 0.05$ or $p < 0.01$.

Results

Isolation and bioinformatics analysis of *PvSVP2*

We isolated two SVP-like genes *PvSVP1* and *PvSVP2*, from *P. violascens* according to the *P. edulis* transcriptome database. However, only *PvSVP2* data were shown in this paper. The *PvSVP2* is 693 bp nucleotides long, and 230 amino acids possess a MADS-box and K-box (Fig. 1a). Moreover, many DNA binding sites and dimerization interfaces were found in the MADS-box of the *PvSVP2* protein (Fig. 1a). Its theoretical molecular weight (MW) and the theoretical isoelectric point (pI) were 26.02 KDa and 7.76, respectively. Phylogenetic tree analysis showed that *PvSVP2* were grouped with monocot Poaceae SVP-

like proteins (Fig.1b). Moreover, PvSVP2 clustered as a subgroup with BM1, ZMM20 and OsMADS47, and was more closely related to OsMADS47 from *O. sativa*, with 75.1% identity (Fig.1c).

Expression analysis of *PvSVP2*

qRT-PCR analysis was carried out for detecting the transcript level of *PvSVP2* in different tissues and developmental stages. The results showed that *PvSVP2* was expressed in all tested tissues, including young leaf, mature leaf, culm, rhizome, shoot and flower (Fig. 2a). In flowering and non-flowering plants, the mRNA levels of *PvSVP2* were higher in culm and rhizome, whereas lowest in the shoot. To determine whether *PvSVP2* were related to flowering in *P. violascens*, we analyzed the expression in the leaf and flower of flowering plant (FL and FF), respectively and the leaf of the non-flowering plant (VL). These tissues were collected in three different stages T1, T2 and T3 as described by our previous publication, Liu et al. (2016) (T1: the time when the floral bud formed and switched from the vegetative phase into the reproductive stage (March 15); T2: The time when the inner organs of the flower began to form (March 29); T3: The blooming stage when the anther was outcropped from palea (April 12)). The expression of *PvSVP2* changed with the flowering stage from March 15 to April 12 (Fig. 2b). The mRNA level of *PvSVP2* in FL increased first from T1 to T2, and then decreased to T3. In VL, the mRNA level of *PvSVP2* was first reduced from T1 to T2 and then remained almost unchanged during T2-T3. In contrast to FL and VL samples, the mRNA level increased significantly from T1 and T2 in FF, then remained unchanged to T3. Moreover, the *PvSVP2* expression in FF was lower at T1 and higher in T2 and T3 than VL and FL (Fig. 2b).

Ectopic expression of *PvSVP2* in *A. thaliana* caused the early flowering and abnormal floral morphologies

To determine *PvSVP2* function, we generated transgenic *A. thaliana* plants expressing *PvSVP2* constitutively (35S::*PvSVP2*). Among eleven homologous T3 transgenic *A. thaliana* lines, we selected three lines (line 1, line 28 and 42) for further analysis. Compared with the wild-type *A. thaliana*, plants carrying 35S::*PvSVP2* vector (line1, line28, and line42) flowered significantly early by an average of 9.4 days (Fig. 3a, b, $p < 0.01$). Further, the number of rosette leaves at the time of bolting for three 35S::*PvSVP2* lines were less than the control plants with an average of 2.4 leaves (Fig. 3c, $p < 0.05$ or $p < 0.01$). The qRT-PCR analysis identified that the flowering time was correlated with the *PvSVP2* expression level (Fig. 3d). For example, line 28 was the earliest flowering plant among the three lines studied, containing the highest transcript level of *PvSVP2*. Moreover, 35S::*PvSVP2* transgenic lines also produced abnormal floral organs. As follow, the sepals of transgenic plants appeared to be small and leaf-like structures (Fig. 4b, c), which did not enclose and protect inner floral parts (Fig. 4e) and kept on until the seed capsule matured (Fig. 4f, g). Meanwhile, the petals also displayed the opened phenotype (Fig. 4a, b). Besides, the petals of 35S::*PvSVP2* transgenic lines were initially green and became purple with the flowering process (Fig. 4b, c).

***PvSVP2* overexpression altered the expressions of flowering-related genes in transgenic *A. thaliana* plants**

It is well reported that *SOC1*, *FT* and *FLC* genes are involved in the regulation of flowering time (Li et al. 2008; Jang et al. 2009; Mateos et al. 2015). Therefore, to analyze the influence of *PvSVP2* on the flowering time, transcript levels of *FT*, *SOC1* and *FLC* genes were analyzed by qRT-PCR. Compared with the wild-type plants, in *35S::PvSVP2* transgenic plants, *FT* and *SOC1* transcript levels were both increased, but *FLC* transcript levels displayed no noticeable change (Fig. 5). These results indicate that *PvSVP2* overexpression causes early flowering mainly by upregulating the *FT* and *SOC1* genes in transgenic *A. thaliana*. Further, we also analyzed the *AP1*, *AP3* and *PI* genes, which are essential for developing flower organs (Liu et al. 2009). The *AP1*, *AP3* and *PI* expressions were highly upregulated in *35S::PvSVP2* transgenic plants compared with the wild-type plants. The qRT-PCR results indicated that *AP1*, *AP3* and *PI* expressions are positively correlated with *PvSVP2* expression in transgenic lines (Fig. 5). These results indicated that overexpression of *PvSVP2* in *A. thaliana* affects the development of the floral organ by modulating *AP1*, *AP3* and *PI* expression.

PvSVP2 located in the nucleus and cytomembrane

We predicted that the *PvSVP2* was located in the nucleus by the WoLF PSORT software. Further, we confirmed the subcellular location using the particle bombardment method using onion epidermal cells. Confocal microscope images revealed that the *PvSVP2*-GFP fusion protein was mainly localized in the nucleus and thinly localized in the cytomembrane of the onion epidermal cells. In contrast, the empty vector was uniformly distributed throughout the whole onion cell (Fig. 6a). To further confirm this, the *PvSVP2*-GFP fusion vector was also transformed into the *A. thaliana* protoplasts by PEG-mediated transformation. These results also confirm that *PvSVP2*-GFP was positioned in the nucleus and cytomembrane of the *A. thaliana* protoplasts (Fig. 6b).

PvSVP2 could interact with PvVRN1 and PvMADS56 in yeast two-hybrid and BIFC assays

To further investigate the *PvSVP2* role in flowering, the protein-protein interaction experiments were performed between *PvSVP2* and *PvVRN1* (an *AP1* homolog) (Ma et al. 2016) and *PvMADS56* (a *SOC1* homolog) (Liu et al. 2016) through yeast two-hybrid. The *PvSVP2*, *PvVRN1* and *PvMADS56* genes in pGBKT7 or pGADT7 developed white colonies in SD/-Leu/X-gal or SD/-Trp/X-gal media, respectively, suggesting that these proteins had no transcriptional activity in yeast (Fig. S1). The yeast cells co-transformed with pGBKT7-*PvSVP2* + pGADT7-*PvVRN1* and pGBKT7-*PvSVP2* + pGADT7-*PvMADS56* were able to develop blue colonies in SD/-Trp/-Leu/-His/-Ade/ X- α -gal media (Fig. 7). These results indicated the direct *PvSVP2* interaction with *PvVRN1* and *PvMADS56* in yeast cells. Further, we confirmed these protein-protein interactions through BIFC assay. Strong YFP signals were observed in the cytoplasm of protoplasts transformed with plasmids *PvSVP2*-cYFP/*PvMADS56*-nYFP and *PvSVP2*-cYFP/*PvVRN1*-nYFP (Fig. 8). BIFC experiment confirmed that *PvSVP2* could interact with *PvVRN1*, *PvMADS56* in vivo.

Prokaryotic expression of PvSVP2

We used the prokaryotic expression system to analyze *PvSVP2* protein solubility. The *PvSVP2*-pHTT construct was induced at 37°C and 20°C, respectively (Fig. 9a). SDS-PAGE analysis showed that a

specific protein band of about 30 kDa was expressed in supernatant at 20°C by IPTG induction (Fig. 9a, lane 5). However, the molecular mass of the fusion protein was 27 kDa including a 1kDa His tag protein and a 26 kDa PvSVP2 protein. To further verify it, the soluble protein was further purified with a dextrin sepharose high performance Fig. 9b) and the protein sequence was examined by MALDI-TOF/TOF mass spectrometer analysis. As Fig. 9c shown, the generated peptides and the peptides derived from PvSVP2 protein sequence had high coverage rate, reach to 53%, indicating that the protein was PvSVP2-pHTT fusion protein.

Discussion

The *SVP* genes play a crucial role in controlling flowering time and floral organ characteristics (Hartmann et al. 2000; Michaels et al. 2003). In this study, we isolated and characterized one *SVP* homolog, *PvSVP2*, from Lei bamboo. Phylogenetic analysis showed that *PvSVP2* belonged to the same group with *BM1*, *ZMM20* and *OsMADS47* from monocot plants and was closely related to *OsMADS47* (Figure 1b, c). Previous studies indicate that *SVP* homologs are different and have three types of expression patterns. The first type is mainly expressed in vegetative tissues but not in reproductive tissues like *AtSVP* (Hartmann et al. 2000), *BM1* (Trevaskis et al. 2007), *OsMADS47* (Lee et al. 2012) and *AcSVPs* (Wu et al. 2012; Wu et al. 2017); the second type is expressed in reproductive tissues but not in vegetative tissues such as *OsMADS22* (Lee et al. 2012); the third type is expressed both in vegetative and reproductive tissues such as *OsMADS55* (Lee et al. 2012), *INCOMPOSITA* (Masiero et al. 2004), *MtSVP* (Jaudal et al. 2014), *CmSVP* (Gao et al. 2017), *LoSVP* (Tang et al. 2020), *EiSVPs* (Jiang et al. 2019), *MiSVPs* (Mo et al. 2021) and *PavSVP* (Wang et al. 2021). Our results identified that *PvSVP2* belongs to the third type and was expressed in all vegetative and reproductive tissues such as leaf, culm, rhizome, shoot and flower (Figure 2). These results showed that the expression pattern of *SVP*-like genes is various, suggesting that their function may be different in different species.

To identify its function, *PvSVP2* was ectopically expressed in *A. thaliana*. The *35S::PvSVP2* transgenic plants displayed abnormal sepal and petal structures (Fig. 4). These phenotypic observations were consistent with most *SVP*-group MADS-box genes studied. It was worth noting that the petals of these transgenic plants became purple in color. Similar phenotype was observed in *A. thaliana* transgenic plants overexpressed with the *OsMADS22* gene (Fornara et al. 2008). Despite this, *PvSVP2* was closely related to *OsMADS47* rather than *OsMADS22*. For *SVP* homologs, most of them mainly as a repressor in regulating flowering time, but recent studies find that a few have opposite function. For example, *PfMADS16* (*Polypogon fugax*) and *MiSVP2* overexpressing in *A. thaliana* displayed an early flowering phenotype (Mo et al. 2021; Zhou et al. 2020). Our results also show that overexpression of *PvSVP2* led to early flowering in transgenic *A. thaliana* lines (Fig. 3a-c). These results suggested that *SVP*-like genes have functional conservation and diversification.

Because the overexpression of *PvSVP2* resulted in early flowering and abnormal organs, the transcript levels of related genes were analyzed in *35S::PvSVP2* plants. The qRT-PCR results showed that the *FT* and *SOC1* gene expression was significantly increased and positively correlated with *PvSVP2* expression

in transgenic lines (Fig. 5). These results were consistent with overexpression studies of *MiSVP2* and *PfMADS16* in *A. thaliana*, which displayed an early flowering phenotype (Mo et al. 2021; Zhou et al. 2020). But unlike *MiSVP2*, the expression of *FLC* remained unaltered in *35S::PvSVP2* transgenic plants. Moreover, *AP1*, *AP3* or *PI* expressions were increased in these transgenic plants (Fig. 5). In conclusion, *PvSVP2* affected flowering time by regulating *FT* and *SOC1* expression and flower development by regulating *AP1*, *AP3* and *PI* expression in transgenic *A. thaliana* plants.

In *A. thaliana*, SVP can interact with SOC1 or AP1 protein to regulate flowering time and to establish floral meristem identity, respectively (Gregis et al. 2008; Lee et al. 2008b). In this study, PvSVP2 could interacted with PvMADS56 and PvVRN1 as demonstrated by the yeast two-hybrid and BiFC assays (Fig. 7, 8). *PvMADS56* (a *SOC1* homolog) and *PvVRN1* (an *AP1* homolog) from *P. violascens* overexpressing in *A. thaliana* display not only abnormal floral organs but also caused early flowering (Liu et al. 2016; Ma et al. 2016). Therefore, we proposed that *PvSVP2* might affect flowering time and flower development by interacting with *PvVRN1* and *PvMADS56* in bamboo.

SVP and SOC1 are located in the nucleus and cytoplasm, respectively. However, SOC1-SVP heterodimers are translocated to the nucleus, suggesting SOC1 localization is affected by SVP (Lee et al. 2008b). Unlike SVP, PvSVP2 is not only located in the nucleus but also in the cytomembrane (Fig. 6). The same results are found for the subcellular location of PavSVP (Wang et al. 2021). Intriguingly, PvMADS56-PvSVP2 and PvVRN1-PvSVP2 heterodimers were translocated to the cytoplasm by transient assays, whereas PvMADS56 and PvVRN1 are also located in the nucleus (Fig. 8) (Liu et al. 2016; Ma et al. 2016). These data suggested that *PvSVP2* was different from *SVP* in signal transduction and needed a further study for confirmation. Besides, with the success of prokaryotic expression in this paper, these results will be helpful for further functional research of *PvSVP2* in bamboo.

Declarations

Author contribution statement Shina Liu designed and performed all the experiments and write the manuscript. Naresh Vasupalli and Dan Hou revised the manuscript. Xinchun Lin designed the experiments and revised the manuscript.

Funding Our work was funded by National Natural Science Foundation of China (31971735), the Natural Science Foundation of Zhejiang Province (LZ20C160002) and the State Key Laboratory of Subtropical Silviculture (ZY20180203).

Conflicts of interest The authors declare no conflict of interest.

References

1. Amasino RM, Michaels SD (2010) The Timing of Flowering. *Plant Physiol* 154: 516-520
2. Andrés F, Porri A, Torti S, Mateos J, Romera-Branchat M, García-Martínez JL, Fornara F, Gregis V, Kater MM, Coupland G (2014) *SHORT VEGETATIVE PHASE* reduces gibberellin biosynthesis at the

- Arabidopsis* shoot apex to regulate the floral transition. PANS 111: E2760-E2769
3. Bouché F, Lobet G, Tocquin P, Périlleux C (2015) FLOR-ID: An interactive database of flowering-time gene networks in *Arabidopsis thaliana*. Nucleic Acids Res 44: D1167-D1171
 4. de Folter S, Immink RGH, Kieffer M, Pařenicová L, Henz SR, Weigel D, Busscher M, Kooiker M, Colombo L, Kater MM, Davies B, Angenent GC (2005) Comprehensive Interaction Map of the *Arabidopsis* MADS Box Transcription Factors. The Plant Cell 17: 1424-1433
 5. Fornara F, Gregis V, Pelucchi N, Colombo L, Kater M (2008) The rice *StMADS11*-like genes *OsMADS22* and *OsMADS47* cause floral reversions in *Arabidopsis* without complementing the *svp* and *agl24* mutants. J Exp Bot 59: 2181-219
 6. Gao Y, Gao Y, Fan M, Yuan L, Wu Z, Zhang Q (2017) Overexpression of *Chrysanthemum morifolium* *SVP* gene delays blossoming and regulates inflorescence architecture in transgenic *Arabidopsis*. Can J Plant Sci 97: 1130-1139
 7. Gregis V, Sessa A, Colombo L, Kater MM (2006) *AGL24*, *SHORT VEGETATIVE PHASE*, and *APETALA1* Redundantly Control *AGAMOUS* during Early Stages of Flower Development in *Arabidopsis*. The Plant Cell 18: 1373-1382
 8. Gregis V, Sessa A, Colombo L, Kater MM (2008) *AGAMOUS-LIKE24* and *SHORT VEGETATIVE PHASE* determine floral meristem identity in *Arabidopsis*. The Plant J 56: 891-902
 9. Hartmann U, Hohmann S, Nettesheim K, Wisman E, Saedler H, Huijser P (2000) Molecular cloning of *SVP*: a negative regulator of the floral transition in *Arabidopsis*. The Plant J 21: 351-360
 10. Hou D, Li L, Ma T, Pei J, Zhao Z, Lu M, Wu A, Lin X (2021) The *SOC1*-like gene *BoMADS50* is associated with the flowering of *Bambusa oldhamii*. Horticulture Research 8: 1-13
 11. Hou D, Zhao Z, Hu Q, Li L, Vasupalli N, Zhuo J, Zeng W, Wu A, Lin X (2020) *PeSNAC-1*, a NAC transcription factor from moso bamboo (*Phyllostachys edulis*) confers tolerance to salinity and drought stress in transgenic rice. Tree Physiol 40: 1792-1806
 12. Jang S, Torti S, Coupland G (2009) Genetic and spatial interactions between *FT*, *TSF* and *SVP* during the early stages of floral induction in *Arabidopsis*. The Plant J 60: 614-625
 13. Jaudal M, Monash J, Zhang L, Wen J, Mysore KS, Macknight R, Putterill J (2013) Overexpression of Medicago *SVP* genes causes floral defects and delayed flowering in *Arabidopsis* but only affects floral development in Medicago. J Exp Bot 65:429-442
 14. Jiang Y, Peng J, Zhang Z, Lin S, Lin S, Yang X (2019) The Role of *EjSVPs* in Flower Initiation in *Eriobotrya japonica*. Int J Mol Sci 20: 5933
 15. Lee S, Choi SC, An G (2008a) Rice *SVP*-group MADS-box proteins, *OsMADS22* and *OsMADS55*, are negative regulators of brassinosteroid responses. The Plant J 54: 93-105
 16. Lee J, Oh M, Park H, Lee I (2008b) *SOC1* translocated to the nucleus by interaction with *AGL24* directly regulates *LEAFY*. The Plant J 55: 832-43
 17. Lee JH, Park SH, Ahn JH (2012) Functional conservation and diversification between rice *OsMADS22*

18. *OsMADS55* and *ArabidopsisSVP* proteins. *Plant Sci* 185: 97-104
19. Lee JH, Ryu H-S, Chung KS, Posé D, Kim S, Schmid M, Ahn JH (2013) Regulation of Temperature-
20. Responsive Flowering by MADS-Box Transcription Factor Repressors. *Science* 342: 628-632
21. Li D, Liu C, Shen L, Wu Y, Chen H, Robertson M, Helliwell CA, Ito T, Meyerowitz E, Yu H (2008) A Repressor Complex Governs the Integration of Flowering Signals in *Arabidopsis*. *Dev Cell* 15: 110-120
22. Li ZM, Zhang JZ, Mei L, Deng XX, Hu CG, Yao JL (2010) PtSVP, an SVP homolog from trifoliate orange (*Poncirus trifoliata* L. Raf.), shows seasonal periodicity of meristem determination and affects flower development in transgenic *Arabidopsis* and tobacco plants. *Plant Mol Biol* 74: 129-23. 142
24. Lin SY, Mao GX (2007) The habit and regeneration of bamboo flowering (In Chinese). *For Sci Technol* 32: 23-25
25. Liu S, Qi T, Ma J, Ma T, Ma L, Lin X (2016) Ectopic expression of a *SOC1* homolog from *Phyllostachys violascens* alters flowering time and identity of floral organs in *Arabidopsis thaliana*. *Trees* 30: 2203-2215
26. Liu C, Xi W, Shen L, Tan C, Yu H (2009) Regulation of Floral Patterning by Flowering Time Genes. *Dev Cell* 16: 711-722
27. Livak KJ, Schmittgen TD (2001) Analysis of Relative Gene Expression Data Using Real-Time Quantitative PCR and the $2^{-\Delta\Delta CT}$ Method. *Methods* 25: 402-408
28. Ma JJ, Liu SN, Zhu LF, Qi TT, Lin XC (2016) Cloning and functional analysis of *VRN1* gene from
29. *Phyllostachys violascens* (In Chinese). *Journal of nuclear agricultural sciences* 30: 1699-1705
30. Marín-González E, Matías-Hernández L, Aguilar-Jaramillo AE, Lee JH, Ahn JH, Suárez-López P, Pelaz S (2015) SHORT VEGETATIVE PHASE Up-Regulates TEMPRANILLO2 Floral Repressor at Low Ambient Temperatures. *Plant Physiol* 169: 1214-1224
31. Masiero S, Li M-A, Will I, Hartmann U, Saedler H, Huijser P, Schwarz-Sommer Z, Sommer H (2004) *INCOMPOSITA*: a MADS-box gene controlling prophyll development and floral meristem identity in *Antirrhinum*. *Development* 131: 5981-5990
32. Mateos JL, Madrigal P, Tsuda K, Rawat V, Richter R, Romera-Branchat M, Fornara F, Schneeberger K, Krajewski P, Coupland G (2015) Combinatorial activities of *SHORT VEGETATIVE PHASE* and *FLOWERING LOCUS C* define distinct modes of flowering regulation in *Arabidopsis*. *Genome Biol* 16: 31
33. Michaels SD, Ditta G, Gustafson-Brown C, Pelaz S, Yanofsky M, Amasino RM (2003) *AGL24* acts as a promoter of flowering in *Arabidopsis* and is positively regulated by vernalization. *The Plant J* 33: 867-874
34. Parcy F (2005) Flowering: a time for integration. *Int J Dev Biol* 49: 585-593
35. Peng Z, Lu Y, Li L, Zhao Q, Feng Q, Gao Z, Lu H, Hu T, Yao N, Liu K, Li Y, Fan D, Guo Y, Li W, Lu Y, Weng Q, Zhou C, Zhang L, Huang T, Zhao Y, Zhu C, Liu X, Yang X, Wang T, Miao K, Zhuang C, Cao X, Tang

- W, Liu G, Liu Y, Chen J, Liu Z, Yuan L, Liu Z, Huang X, Lu T, Fei B, Ning Z, Han B, Jiang Z (2013) The draft genome of the fast-growing non-timber forest species moso bamboo (*Phyllostachys heterocyclus*). *Nat Genet* 45: 456-461
36. Qi FY; Hu T; Peng ZH; Gao J (2013) Screening of reference genes used in qRT-PCR and expression analysis of *PheTFL1* gene in Moso Bamboo (In Chinese). *Acta Bot Borea* 33: 0048-0052
37. Sentoku N, Kato H, Kitano H, Imai R (2005) OsMADS22, an STMADS11-like MADS-box gene of rice, is expressed in non-vegetative tissues and its ectopic expression induces spikelet meristem indeterminacy. *Mol Genet Genomics* 273: 1-9
38. Sharma P, Dhanwantri K, Mehta S (2014) Bamboo as a building material. *Int J Civ Eng* 5: 249-254
39. Tamura K, Peterson D, Peterson N, Stecher G, Nei M, Kumar S (2011) MEGA5: Molecular Evolutionary Genetics Analysis Using Maximum Likelihood, Evolutionary Distance, and Maximum Parsimony Methods. *Mol Biol Evol* 28: 2731-2739
40. Tang X, Liang M, Han J, Cheng J, Zhang H, Liu X (2019) Ectopic expression of *LoSVP*, a MADS-domain transcription factor from lily, leads to delayed flowering in transgenic *Arabidopsis*. *Plant Cell Rep* 39: 289-298
41. Trevaskis B, Tadege M, Hemming MN, Peacock WJ, Dennis ES, Sheldon C (2006) Short Vegetative Phase-Like MADS-Box Genes Inhibit Floral Meristem Identity in Barley. *Plant Physiol* 143: 225-235
42. Wang J, Jiu S, Xu Y, Sabir IA, Wang L, Ma C, Xu W, Wang S, Zhang C (2021) SVP-like gene *PavSVP* potentially suppressing flowering with *PavSEP*, *PavAP1*, and *PavJONITLESS* in sweet cherries (*Prunus avium* L.). *Plant Physiol Bioch* 159: 277-284
43. Wang YC, Klein TM, Fromm M, Cao J, Sanford JC, Wu R (1988) Transient expression of foreign genes in rice, wheat and soybean cells following particle bombardment. *Plant Mol Biol* 11: 433-439
44. Wu RM, Walton EF, Richardson AC, Wood M, Hellens RP, Varkonyi-Gasic E (2011) Conservation and divergence of four kiwifruit *SVP*-like MADS-box genes suggest distinct roles in kiwifruit bud dormancy and flowering. *J Exp Bot* 63: 797-807
45. Wu R, Wang T, Warren BAW, Allan AC, Macknight RC, Varkonyi-Gasic E (2017) Kiwifruit *SVP2* gene prevents premature budbreak during dormancy. *J Exp Bot* 68: 1071-1082
46. Yao W, Li C, Lin S, Ren L, Wan Y, Zhang L, Ding Y (2020) Morphological Characteristics and Transcriptome Comparisons of the Shoot Buds from Flowering and Non-Flowering *Pleiblastus pygmaeus*. *Forests* 11: 1229
47. Yoo SD, Cho YH, Sheen J (2007) *Arabidopsis* mesophyll protoplasts: a versatile cell system for transient gene expression analysis. *Nature Protocols* 2: 1565-1572
48. Zheng X, Lin S, Fu H, Wan Y, Ding Y (2020) The Bamboo Flowering Cycle Sheds Light on Flowering Diversity. *Front Plant Sci* 11: 381
49. Zhou FY, Yu Q, Zhang Y, Yao CC, Han YJ (2020) StMADS11 Subfamily Gene *PfMADS16* From *Polypogon fugax* Regulates Early Flowering and Seed Development. *Front Plant Sci* 11: 525

Figures

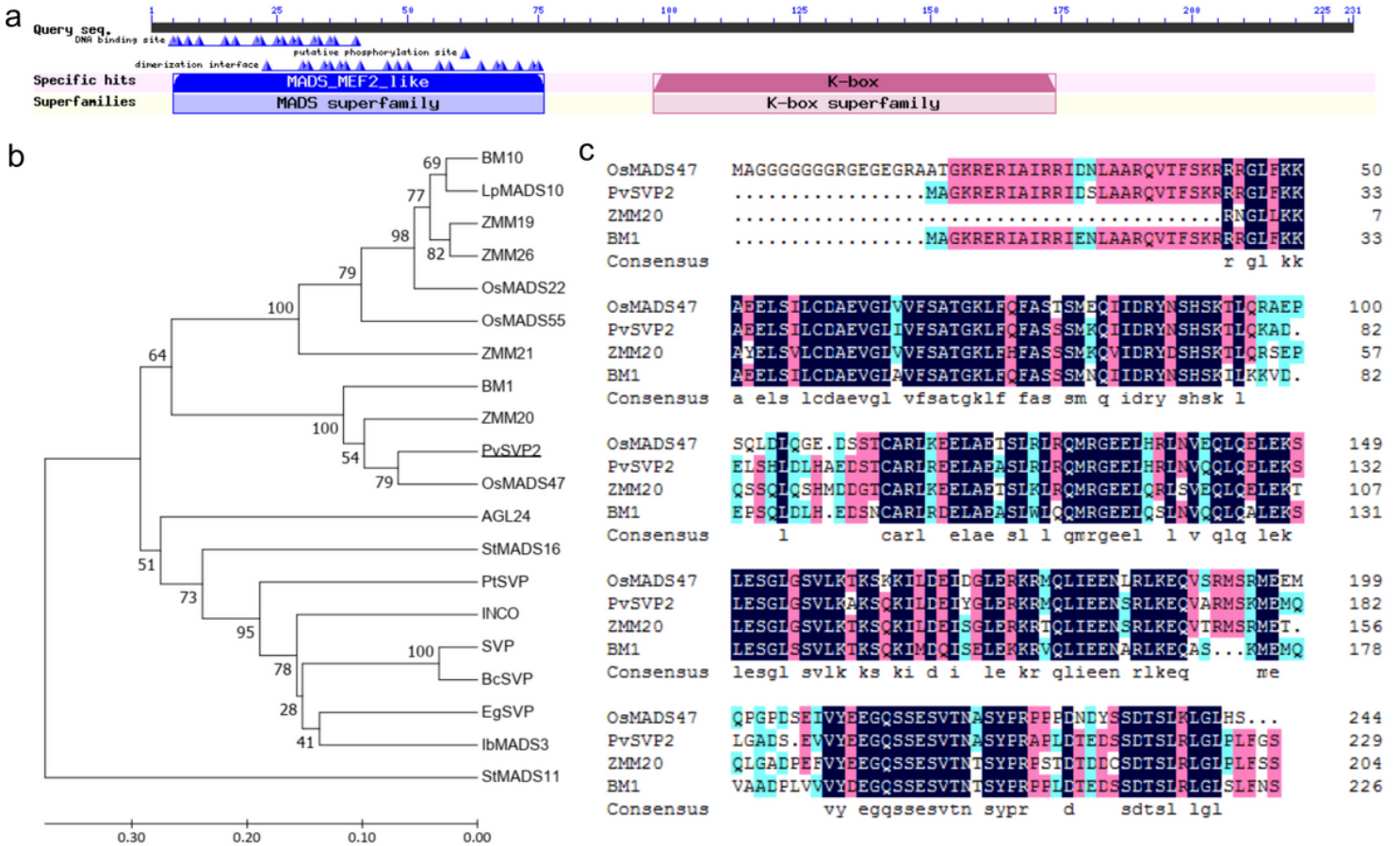


Figure 1

Sequence analysis of PvSVP2. **a** Prediction of PvSVP2 by NCBI Conserved Domain database (<https://www.ncbi.nlm.nih.gov/Structure/cdd/wrpsb.cgi>). **b** Phylogenetic analysis of PvSVPs and their orthologs from other plant species. Amino acid sequences were aligned using Clustal W, and the tree was constructed using the neighbor-joining method by bootstrap with 1000 replicates in Mega 5.0. SVP-like proteins source and GenBank accession number: BM1: *Hordeum vulgare* (CAB97350); BM10: *Hordeum vulgare* (ABM21529); LpMADS10: *Lolium perenne* (AAZ17549); ZMM19: *Zea mays* (AJ430633); ZMM20: *Zea mays* (AJ430634); ZMM21: *Zea mays* (AJ430635); ZMM26: *Zea mays* (AJ430693); OsMADS22: *O. sativa* (AB107957); OsMADS47 (AAQ23142): *O. sativa* (AAQ23142); OsMADS55: *O. sativa* (BAD35842); StMADS11: *Solanum tuberosum* (AAB94006); StMADS16: *Solanum tuberosum* (AAB94005); EgSVP: *Eucalyptus occidentalis* (AAP40641); AGL24: *Arabidopsis thaliana* (AEE84922); SVP: *A. thaliana* (NP_179840); BcSVP: *Brassica rapa* (DQ922945); INCO: *Antirrhinum majus* (CAG27846); IbMADS3: *Ipomoea batatas* (AAK27150); PtSVP: *Citrus trifoliata* (ACJ09170). **c** Multiple alignment of the deduced amino acid sequences of PvSVP2, BM1, ZMM20 and OsMADS47.

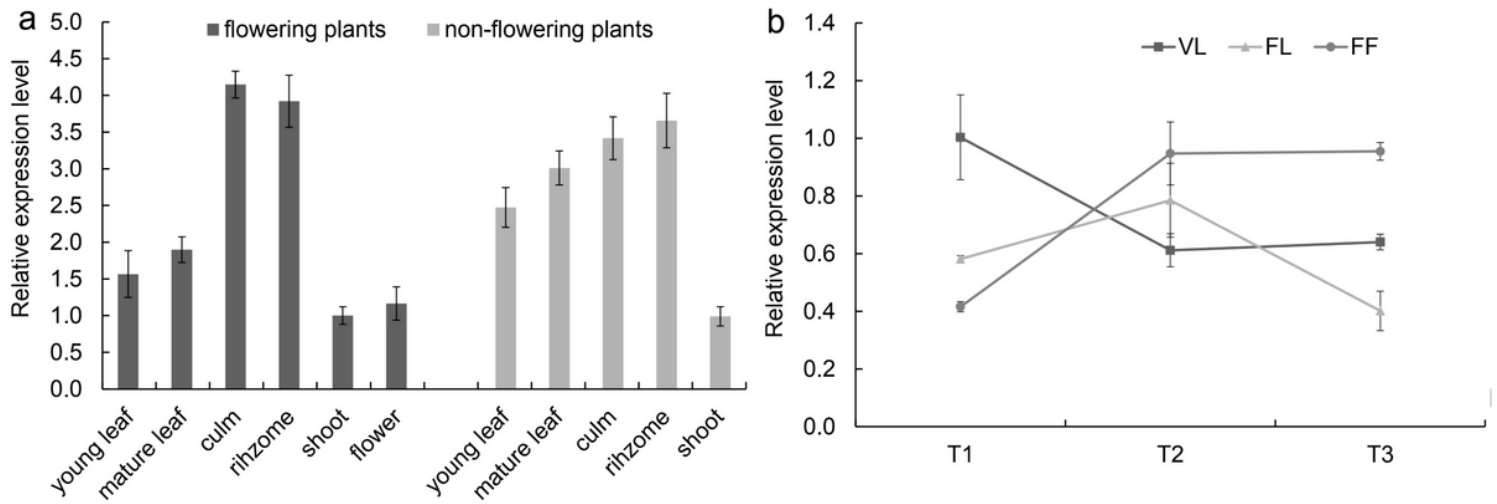


Figure 2

Tissue and temporal expression of *PvSVP2* in flowering and non-flowering *P. violascens*. **a** Relative expression of *PvSVP2* in different tissues. **b** Relative expression of *PvSVP2* in leaves of non-flowering plants (VL), and flowering plants (FL) and flowers (FF) of flowering plants during flower development. Data were mean \pm SE from three biological replicates.

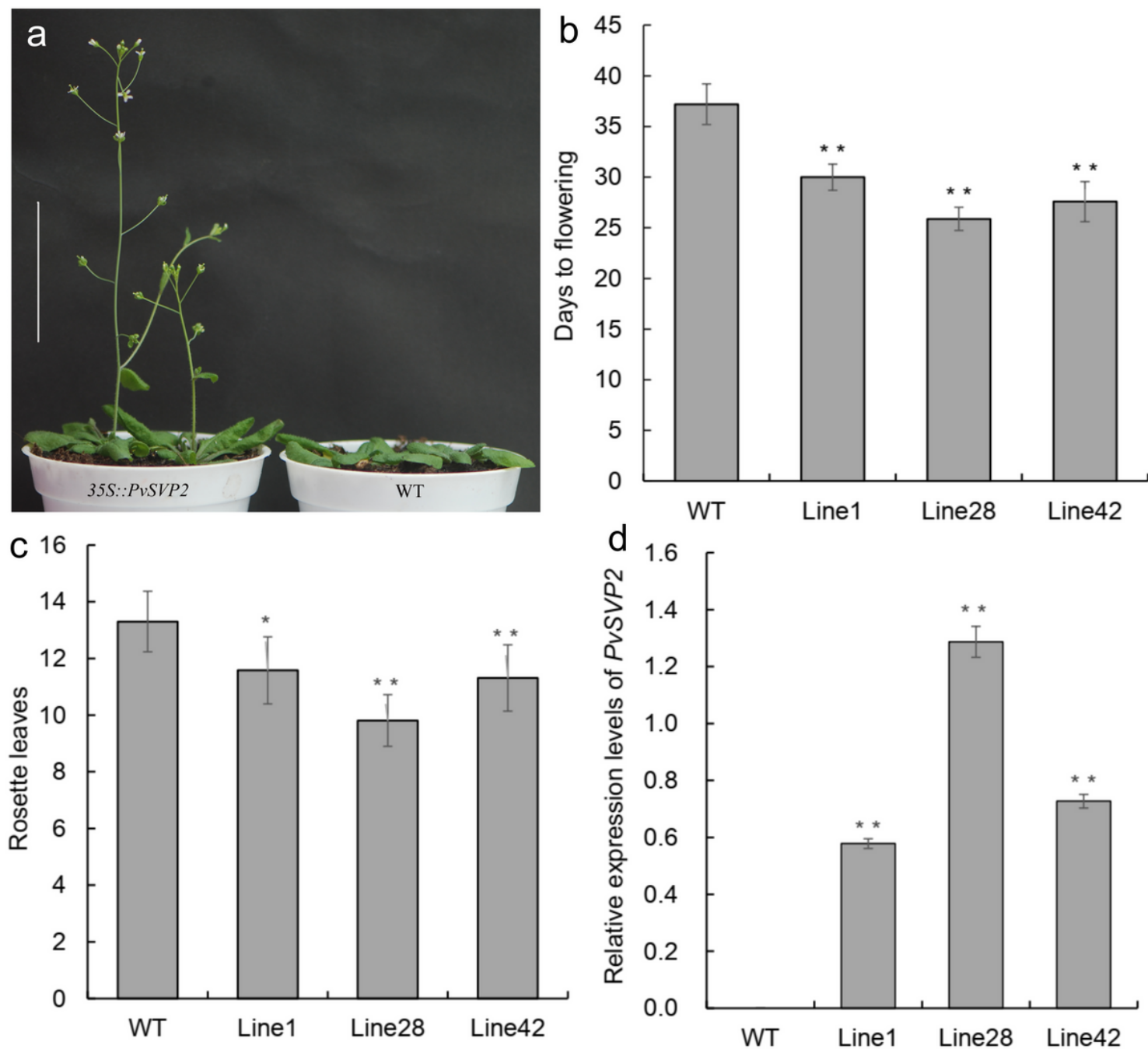


Figure 3

Phenotypic observations and qRT-PCR analysis between transgenic lines (1, 28 and 42) and wild-type (WT) *A. thaliana* plants. **a** The early flowering phenotype of *35S::PvSVP2* transgenic plants. **b** Days to flowering (**c**) number of rosette leaves. **d** Expression analysis of *PvSVP2*. Data were mean \pm SE from three biological replicates. Asterisks indicate significant differences between WT and transgenic plants, $**p < 0.05$ or $**p < 0.01$. The scale bar represents 5 cm.



Figure 4

Flower morphology of wild-type (WT) and *35S::PvSVP2* transgenic *A. thaliana* plants. **a** WT Flower **b** and **c** transgenic flower **d** WT inflorescence **e** transgenic inflorescence **f** siliques of WT **g** siliques of the transgenic plant. The scale bars in Figure represent 1mm.

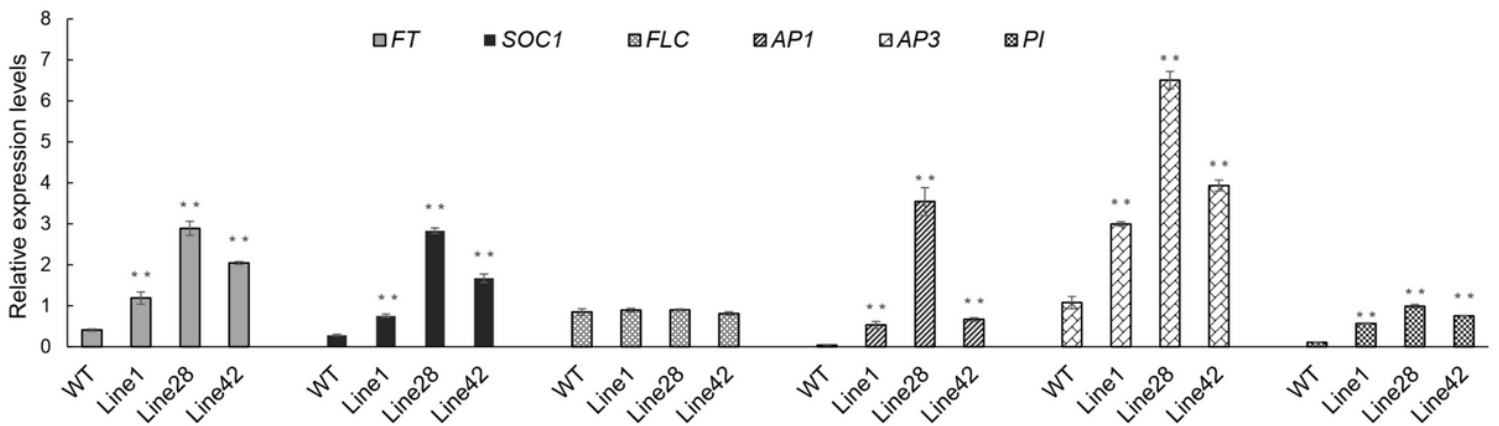


Figure 5

The qRT-PCR results showed that the *FT* and *SOC1* gene expression was significantly increased and positively correlated with *PvSVP2* expression in transgenic lines.

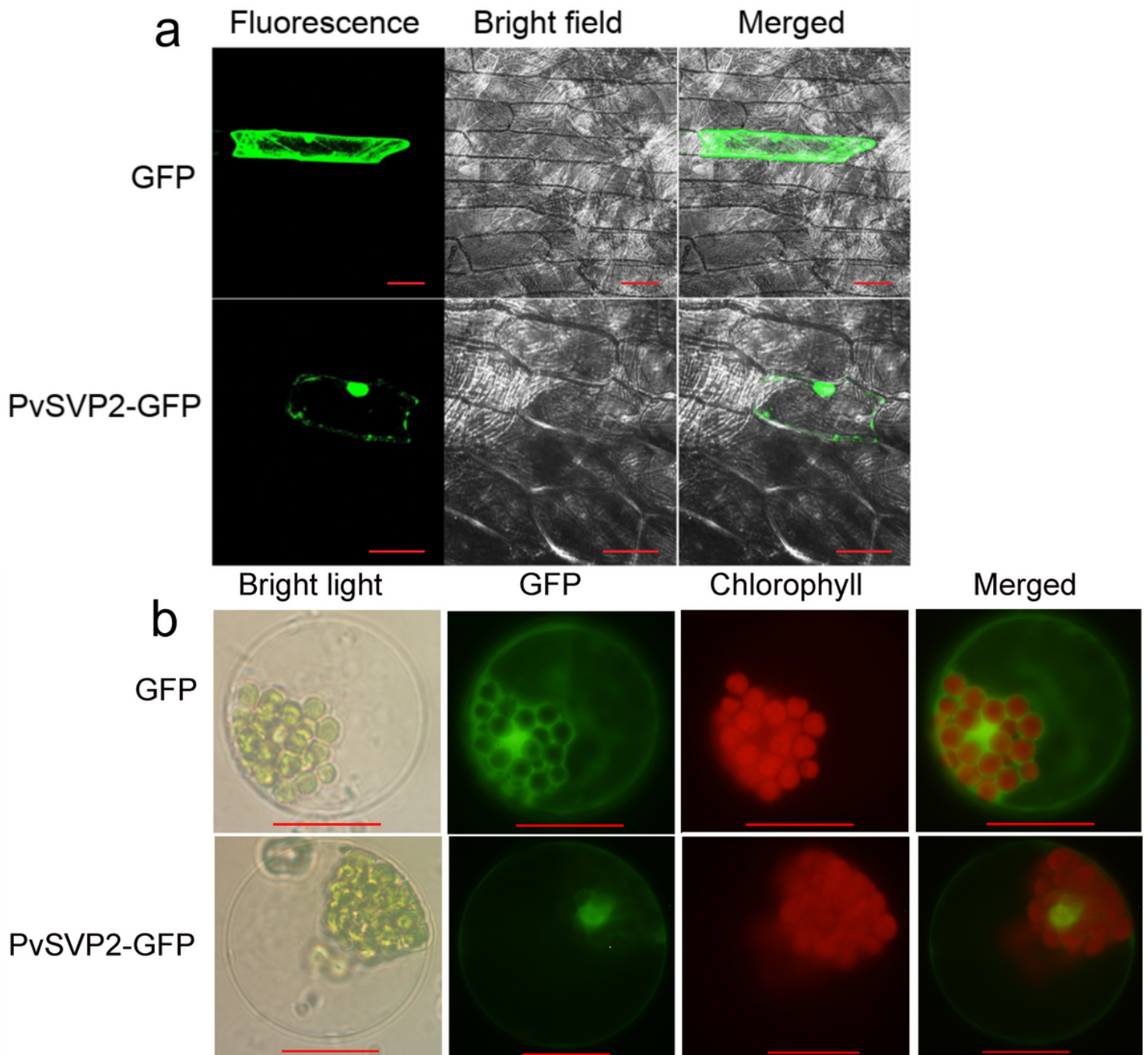


Figure 6

Subcellular location of GFP and PvSVP2-GFP protein in onion cells (a) and *A. thaliana* protoplasts (b). Bars represent 100 μm (a) and 15 μm (b), respectively.

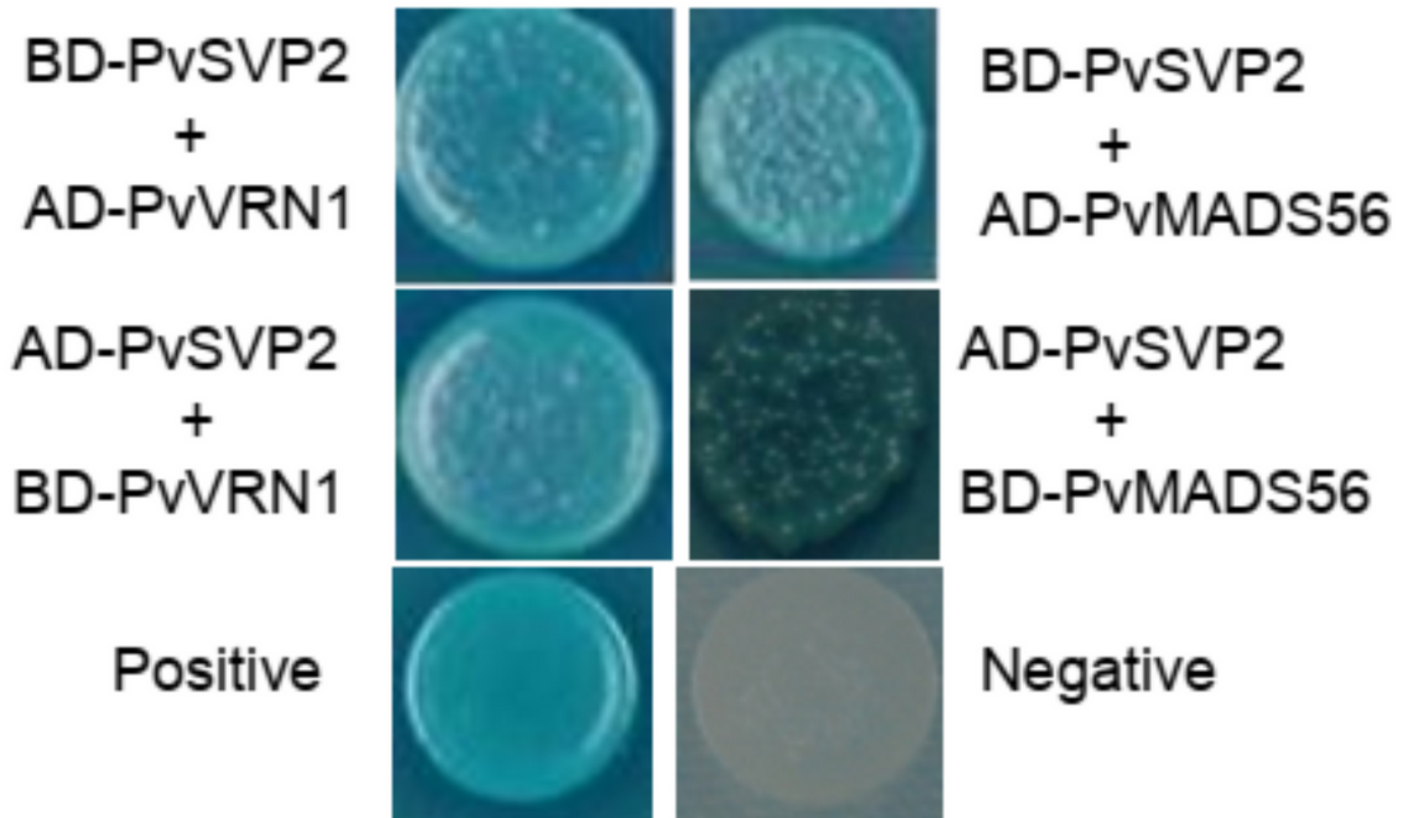


Figure 7

Interactions between PvSVP2 and PvMADS56 or PvVRN1 in yeast two-hybrid experiment. Yeast containing dual vectors of pGBKT7-53 and pGADT7-T was used as the positive control, that of pGBKT7-Lam and pGADT7-T as the negative control. SD/-Leu/-Trp/-His/-Ade medium was used for clone selection purpose. Appearance of X- α -gal activity mirrors positive interaction.

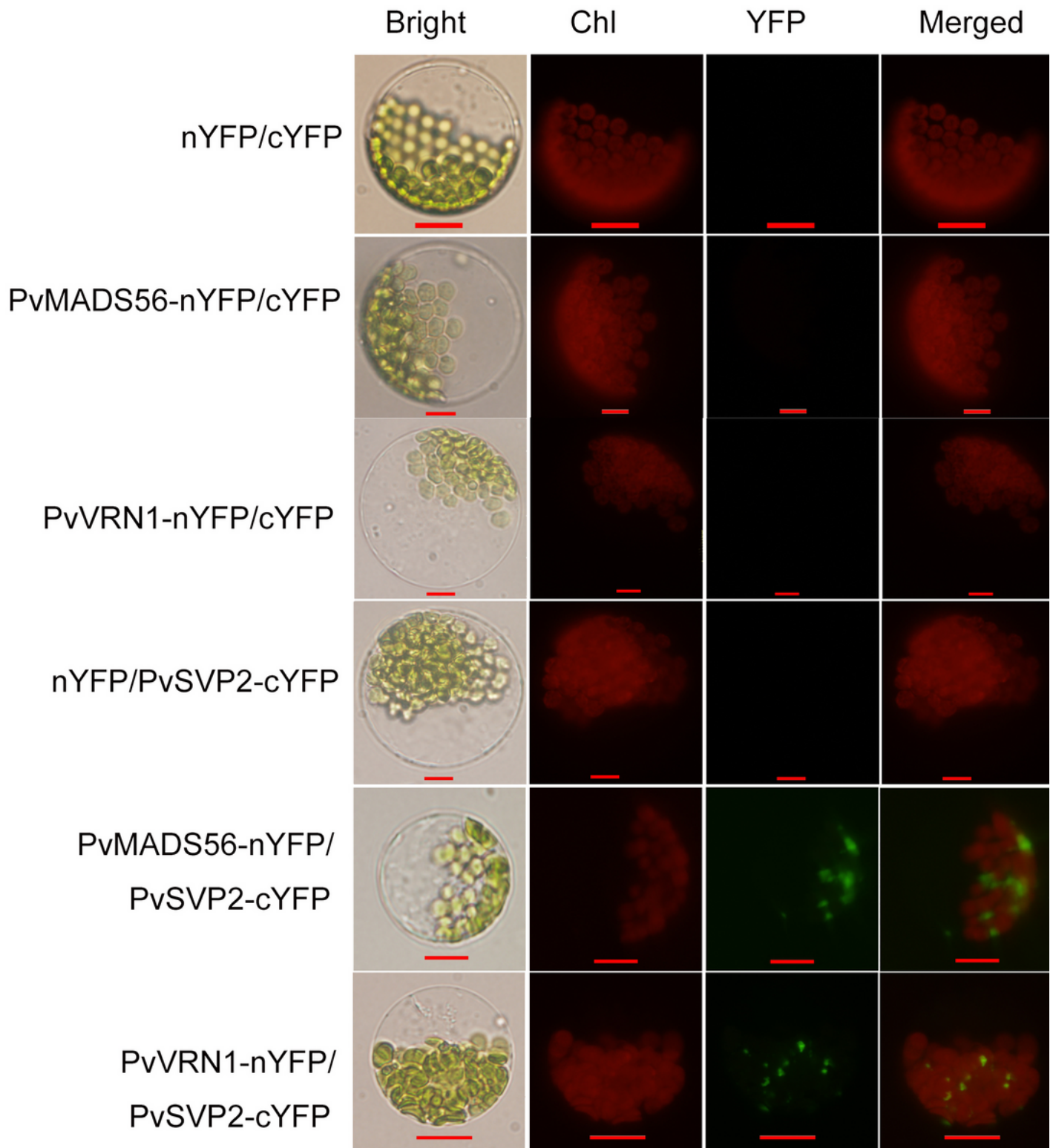


Figure 8

Interactions between PvSVP2 and PvMADS56 or PvVRN1 by BiFC assays. Images were captured 20-h after transient expression under an Olympus confocal microscope. Bars represent 15µm.

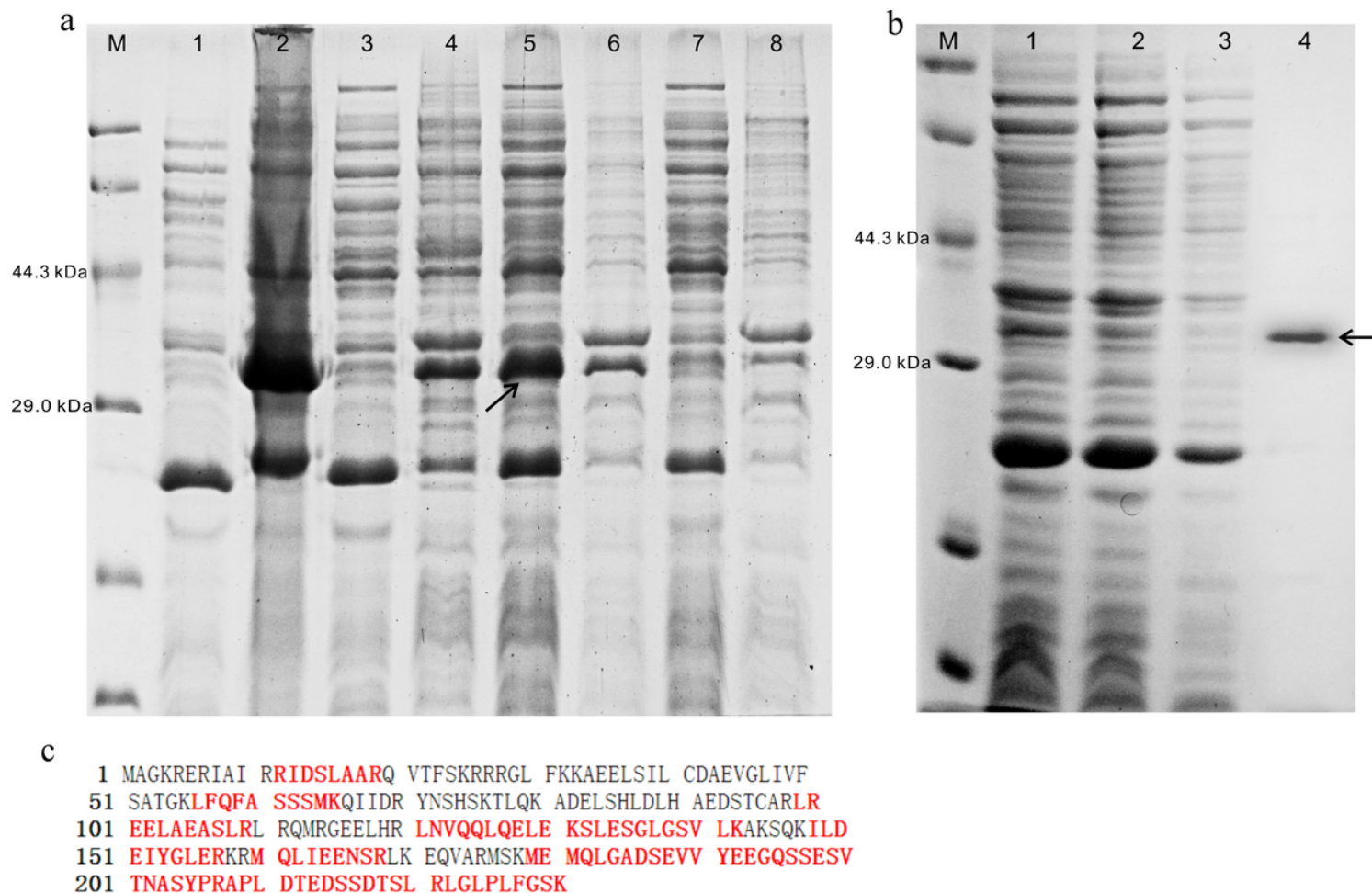


Figure 9

Prokaryotic expression and purification of PvSVP2. **a** SDS-PAGE analysis of PvSVP2 fusion protein in *E. coli* Rosetta (DE3) at 37°C and 20°C. *Lanes* 1, 2, 3, 4 and lanes 5, 6, 7, 8 were respectively at 37°C and 20°C; *lanes* 1, 2, 5, 6 represented the induction with IPTG; *lanes* 3, 4, 7, 8 represented the induction without IPTG. M: marker; *lanes* 1, 3, 5, 7: supernatant; *lanes* 2, 4, 6, 8: precipitation. **b** Purification of PvSVP2. *lane* 1: uninduced; *lane* 2: supernatant after induction; *lane* 3: pellet after induction; *lane* 4: purified PvSVP2 fusion protein by a dextrin sepharose high performance medium. The arrows indicate the position of the fusion protein. **c** MALDI-TOF/TOF mass spectrometer analysis of PvSVP2 fusion protein. The tryptic peptides obtained by mass spectrometry are bold red.

Supplementary Files

This is a list of supplementary files associated with this preprint. Click to download.

- [Fig.S1.jpg](#)
- [TableS1.docx](#)